



Numerical simulation of chaotic maps with the new generalized Caputo-type fractional-order operator

Kolade M. Owolabi ^{a,*}, Edson Pindza ^{b,c}

^a Department of Mathematical Sciences, Federal University of Technology, PMB 704, Akure, Ondo State, Nigeria

^b Department of Mathematics and Applied Mathematics University of Pretoria, Pretoria 002, South Africa

^c Department of Mathematics and Statistics, Tshwane University of Technology, Pretoria West, Pretoria 0183, South Africa

ARTICLE INFO

MSC:

26A33
34A34
35A05
35K57
65L05
65M06
93C10

Keywords:

Chaotic maps
Generalized Caputo-type derivative
Predictor–corrector method
Numerical simulations

ABSTRACT

This work considers a new generalized operator which is based on the application of Caputo-type fractional derivative is applied to model a number of nonlinear chaotic phenomena, such as the Oiseau mythique Bicéphale, Oiseau mythique and L'Oiseau du paradis maps. Numerical approximation of the generalized Caputo-type fractional derivative using the novel predictor–corrector scheme, which indeed is regarded as an extension of a well-known Adams–Bashforth–Moulton classical-order algorithm. A range of new strange chaotic wave propagation was observed for various maps with varying fractional parameters.

Introduction

The application of fractional calculus to model real-life and physical phenomena has been gaining a lot of momentum over the last three decades [1–5]. Fractional calculus is an extension of standard calculus which comprises the derivatives and integrals of integer-order to fractional cases. Much research attention has been paid to the study of fractional differential equations in recent times due to the fact that the fractional-order system response ultimately converges to the integer-order case. The concept of fractional calculus has been used to model various nonlinear dynamical systems, a good example is a chaotic system which has rendered a new dimension to the existing problems. Nowadays, fractional derivatives are used to describe many physical phenomena for the purpose of reliability, better accuracy, and greater flexibility in the model formulation.

A classical order differential operator is called a local operator, while the fractional-order differential operator is referred to as nonlocal derivative due to the fact that the future state not only depends upon the present state but also upon all of the histories of its previous states. For this memory property, the usage of fractional-order models are fast becoming so popular. Fractional differential equations have gained a lot of attention due to their ability to provide an exact description of

different nonlinear scenarios. The main reason that fractional differential equations are being used to model real phenomena is that they are nonlocal in nature, that is, a realistic model of a physical phenomenon depends not only on the time instant but also on the previous time history [6–9]. In addition, fractional derivative serves as a correct tool when it is used to describe the memory and hereditary properties of various materials and processes [1]. In recent years, fractional calculus has been widely used in various applications in almost every field of applied sciences, engineering, and mathematics, and it has gained considerable importance due to its frequent applications in pattern formation (chemical and biological models), fluid flow, polymer rheology, economics, finance, biophysics, control processes, psychology, and chaos theory [10–16].

Over the past few decades, the analysis and application of chaotic phenomena among nonlinear systems have been extensively studied in various disciplines and fields, such as natural science, engineering, social science including psychology and leadership as well as economics and finance. The nonlinear dynamics system consists of three main subgroups, namely: chaos, bifurcation, and soliton. With the inception of nonlinear systems, chaotic dynamics have generated significant attention. Many researchers in various fields, such as biology, chemistry,

* Corresponding author.

E-mail address: kmowolabi@futa.edu.ng (K.M. Owolabi).

physics, mathematics, engineering, and social sciences are currently studying chaotic dynamics [17–21].

In the theory of chaotic dynamics, in order to create chaotic behaviors in the dynamics, it is known and widely believed that the dynamics have to have a third-order system and one nonlinear item at least in a continuous system. For instance, the Lorenz system, Chua’s circuit, Chen system, and Liu system have the third-order systems and one nonlinear item [22–27]. These systems are known to have generated chaotic behaviors with integer-order 3. In the early sixties, attractors were known to represent simple geometric subsets of the phase-space for instance, points, surfaces, lines, and simple regions of three-dimensional space. Later, more studies revealed that complex attractors cannot be classified with such attributes. A proof that some of these physical problems cannot be captured using simple mathematical operators like classical-order differential operator [28–31]. Very strange attractors have been reported including mythical birds, butterfly wings and paradise bird maps [18,32], however, such attractors are still poor and have never been investigated under the framework of the new generalized Caputo-type fractional differential operators. In the present work, the aim is to show via numerical computation that chaotic behaviors can be generated from fractional two-dimensional generalized Oiseau mythique Bicéphale bird map, Oiseau mythique map and L’Oiseau du paradis bird maps involving the generalized Caputo-type fractional-order derivative. Numerical simulations including phase plots considering the predictor–corrector approximation technique. The remaining part of this work is organized into sections. Some useful definitions, properties, and results of the generalized Caputo-type fractional derivative operator are presented in Section “Useful definitions and the new generalized Caputo-type fractional derivative”. Predictor–corrector algorithms are discussed in Section “Predictor-corrector method”. The applicability and suitability of the proposed techniques are tested on some two-dimensional fractional maps systems in Section “Application to chaotic maps problems”. The conclusion is made with the last part.

Useful definitions and the new generalized Caputo-type fractional derivative

In this section, we give some useful definitions and present the new version of the generalized Caputo-type fractional operator [33,34].

Let χ be a function depending on t , the Riemann–Liouville fractional integral of order $\theta > 0$ is mostly defined as

$$\mathcal{I}_{a+}^{\theta} \chi(t) = \frac{1}{\Gamma(\theta)} \int_a^t (t - \xi)^{\theta-1} \chi(\xi) d\xi, \quad t > a. \tag{2.1}$$

The corresponding Caputo and Riemann–Liouville fractional derivatives of order $\theta > 0$ are respectively defined as

$${}^C \mathcal{D}_{a+}^{\theta} \chi(t) = \mathcal{I}_{a+}^{m-\theta} \mathcal{D}^m \chi(t) = \frac{1}{\Gamma(n-\theta)} \int_a^t (t - \xi)^{n-\theta-1} \chi^{(m)}(\xi) d\xi, \quad t > a, \tag{2.2}$$

and

$$R \mathcal{D}_{a+}^{\theta} \chi(t) = \mathcal{I}_{a+}^{m-\theta} \mathcal{D}^m \chi(t) = \frac{1}{\Gamma(m-\theta)} \frac{d^m}{dt^m} \int_a^t (t - \xi)^{m-\theta-1} \chi(\xi) d\xi, \quad t > a, \tag{2.3}$$

where $m - 1 < \theta \leq m$ and $n \in \mathbb{N}$. When $m - 1 < \theta \leq m$, the Caputo derivative satisfies the following rule

$$\mathcal{I}_{a+}^{\theta} {}^C \mathcal{D}_{a+}^{\theta} \chi(t) = \chi(t) - \sum_{j=0}^{m-1} \frac{\chi^{(j)}(a)}{j!} (t - a)^j, \quad t > a. \tag{2.4}$$

It should be mentioned that the Caputo fractional derivative is mostly applied to model many real-life and practical phenomena due to the fact that its most suitable for initial value problems and its very close to classical order derivatives.

Definition 1. The generalized fractional integral of χ , $\mathcal{I}_{a+}^{\theta, \vartheta} \chi(t)$, of order $\theta > 0$ and $\vartheta > 0$ is given by [34]

$$\mathcal{I}_{a+}^{\theta, \vartheta} \chi(t) = \frac{\vartheta^{1-\theta}}{\Gamma\theta} \int_a^t \xi^{\theta-1} (t^\vartheta - \xi^\vartheta)^{\theta-1} \chi(\xi) d\xi, \quad \theta > 0, \quad t > 0. \tag{2.5}$$

Definition 2. The generalized Riemann-type fractional operator with order $\theta > 0$ of the function χ , is defined as [34]

$$R \mathcal{D}_{a+}^{\theta, \vartheta} \chi(t) = \frac{\vartheta^{\theta-m+1}}{\Gamma(m-\theta)} \left(t^{1-\vartheta} \frac{d}{dt} \right)^m \int_a^t \xi^{\theta-1} (t^\vartheta - \xi^\vartheta)^{m-\theta-1} \chi(\xi) d\xi, \tag{2.6}$$

$t > a \geq 0.$

Definition 3. The generalized Caputo-type fractional derivative of a function χ with order $\theta > 0$, is defined as

$${}^C \mathcal{D}_{a+}^{\theta, \vartheta} \chi(t) = \left[R \mathcal{D}_{a+}^{\theta, \vartheta} \left(\chi(s) - \sum_{n=0}^{m-1} \frac{\chi^{(n)}(a)}{n!} (s - a)^n \right) \right] (t), \quad t > a \geq 0, \tag{2.7}$$

where $\theta > 0$ and $m = [\theta]$. If $0 < \theta \leq 1$ and $\chi : [a, b] \rightarrow \mathbb{R}$, where χ is continuous in the interval $[a, b]$, then the above generalized Caputo-type fractional derivative of χ reduces to

$${}^C \mathcal{D}_{a+}^{\theta, \vartheta} \chi(t) = \frac{\vartheta^\theta}{\Gamma(1-\theta)} \int_a^t (t^\vartheta - \xi^\vartheta)^{-\theta} \chi'(\xi) d\xi, \quad 0 < \theta \leq 1, \quad t > a \geq 0. \tag{2.8}$$

The concept of the generalized fractional calculus could be dated to the early 1970 [35]. Details of the existence and uniqueness results for the generalized Caputo-type and Riemann-type fractional derivatives can be found in [33]. The new generalized Caputo-type fractional operator given in [34] is regarded as a modification to the one reported in (2.7). In brief, some of the properties of this new operator will be highlighted here.

By using the generalized integral given in (2.5), the new generalized Caputo-type fractional derivative denoted a $(\mathcal{D}_{a+}^{\theta, \vartheta} \chi)(t) = \left[\mathcal{I}_{a+}^{m-\theta, \vartheta} \mathcal{D}^m (\chi \circ (\vartheta t)^{1/\vartheta}) \right] \left(\frac{t^\vartheta}{\vartheta} \right)$, are given as follows. The new generalized Caputo-type fractional derivative $\mathcal{D}_{a+}^{\theta, \vartheta}$ with order $\theta > 0$ is defined by [34]

$$(\mathcal{D}_{a+}^{\theta, \vartheta} \chi)(t) = \frac{\vartheta^{\theta-m+1}}{\Gamma(m-\theta)} \int_a^t \tau^{\theta-1} (t^\vartheta - \tau^\vartheta)^{m-\theta-1} \left(\tau^{1-\vartheta} \frac{d}{d\tau} \right)^m \chi(\tau) d\tau, \tag{2.9}$$

where $\vartheta > 0, m - 1 < \theta < m$ and $\theta \geq 0$. If in any case $\theta = m$, then

$$(\mathcal{D}_{a+}^{\theta, \vartheta} \chi)(t) = [\mathcal{D}^m (\chi \circ (\vartheta t)^{1/\vartheta})] \frac{t^\vartheta}{\vartheta}.$$

The new generalized Caputo-type fractional derivative above can be applied to model a range of nonlinear phenomena. This new operator is applied to model a range of mythical bird maps in this paper. This new derivative has been proved to satisfy the following properties:

- (a) Assume $a \geq 0, \vartheta > 0, m - 1 < \theta \leq m$ and χ is continuous in the interval $[a, b]$. Then, the relationship between the new generalized Caputo-type fractional derivative (2.9) and the generalized Riemann-type operator (2.6) is expressed by the formula

$$(\mathcal{D}_{a+}^{\theta, \vartheta} \chi)(t) = R \mathcal{D}_{a+}^{\theta, \vartheta} \left(\chi(t) - \sum_{n=0}^{m-1} \frac{1}{\vartheta^n n!} (t^\vartheta - a^\vartheta)^n \left[\left(x^{1-\vartheta} \frac{d}{ds} \right)^n \chi(s) \right] \Big|_{s=a} \right). \tag{2.10}$$

- (b) Assume $a \geq 0, \vartheta > 0, m - 1 < \theta \leq m$ and χ is continuous in the interval $[a, b]$. Then, for $a < t \leq b$, the relationship between the new generalized Caputo-type fractional derivative (2.9) and the generalized integral operator (2.5) satisfies the formula

$$\mathcal{I}_{a+}^{\theta, \vartheta} \mathcal{D}_{a+}^{\theta, \vartheta} \chi(t) = \chi(t) - \sum_{n=0}^{m-1} \frac{1}{\vartheta^n n!} (t^\vartheta - a^\vartheta)^n \left[\left(x^{1-\vartheta} \frac{d}{ds} \right)^n \chi(s) \right] \Big|_{s=a}. \tag{2.11}$$

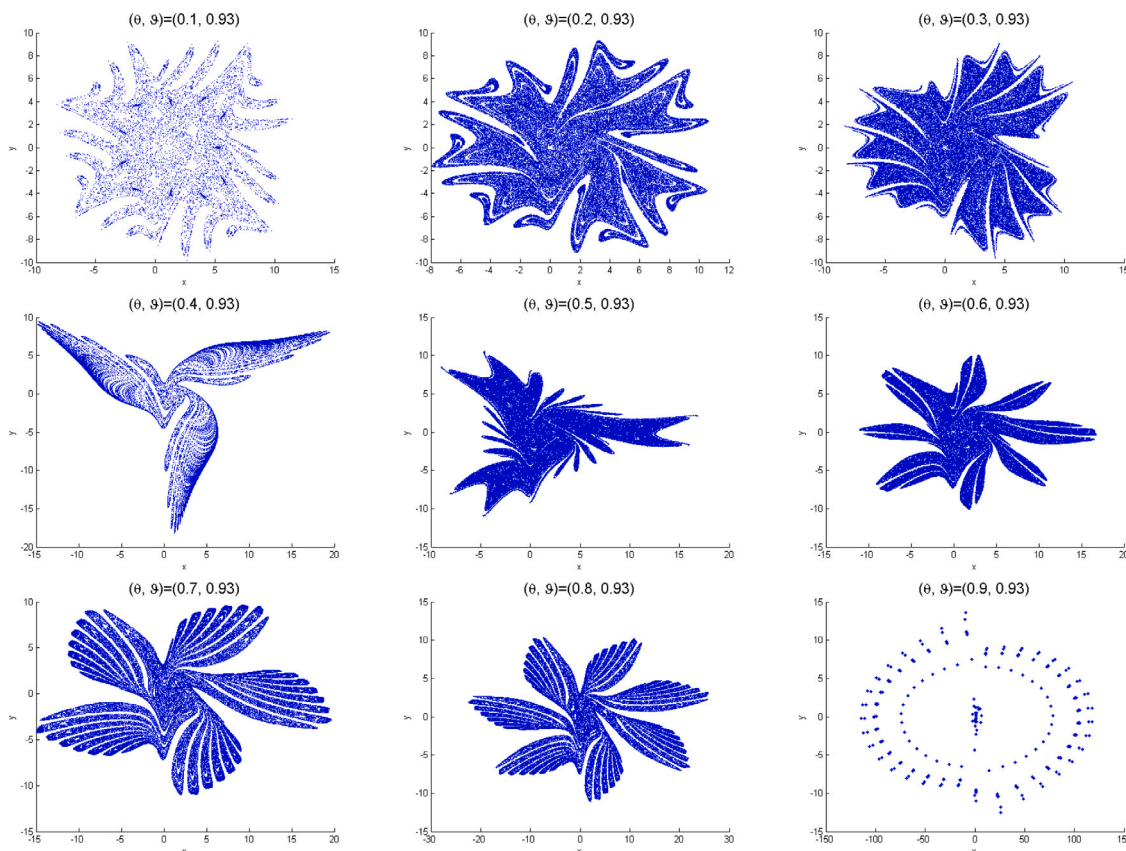


Fig. 1. Numerical simulation for the Oiseau mythique system (4.19) for different values of θ . Simulation runs for $t = 10000$.

(c) Let $a \geq 0, \vartheta > 0, m - 1 < \theta \leq m$ and $\chi \in C[a, b]$. Then, for $a < t \leq b$ the generalized Caputo-type fractional derivative (2.9) is the inverse of the generalized fractional integral operator (2.5)

$$\mathcal{I}_{a+}^{\theta, \vartheta} \mathcal{D}_{a+}^{\theta, \vartheta} \chi(t) = \chi(t). \tag{2.12}$$

As given in properties (a–c), it depicts that the new generalized Caputo-type fractional operator has similar characteristics with the Caputo derivative. Details of formulation and other useful results can be found in [34].

Predictor–corrector method

In this segment, we present and adapt the predictor–corrector method for the solution of general initial value problems which incorporate the generalized Caputo-type fractional derivative. To start with, consider the multidimensional initial value problem written compactly in the form

$${}^C \mathcal{D}_{a+}^{\theta, \vartheta} \omega(t) = g(t, \omega(t)), \quad t \in [0, T], \tag{3.13}$$

subject to initial conditions

$$\omega^\sigma(a) = \omega_0^\sigma, \quad \sigma = 0, 1, 2, \dots, [\theta] \tag{3.14}$$

where ${}^C \mathcal{D}_{a+}^{\theta, \vartheta}$ is the generalized Caputo-type fractional derivative operator as earlier defined with $a > 0$ and $\theta > 0$, $g(t, \omega(t))$ is the linear or nonlinear reaction kinetics. Under some weak conditions on the function g , one can say that a solution exists and that this solution is uniquely determined. The real numbers $\omega_0^{(\sigma)}$ are assumed to be given. By applying property (2.11), if $\vartheta > 0, m - 1 < \theta \leq m$ and $\omega \in C^m[a, T]$, the initial value problem (3.13) together with (3.14) can be written in the integral form

$$\omega(t) = \mu(t) + \frac{\vartheta^{1-\theta}}{\Gamma(\theta)} \int_a^t \tau^{\vartheta-1} (t-\tau)^{\theta-1} g(\tau, \omega(\tau)) d\tau, \tag{3.15}$$

where

$$\mu(t) = \sum_{n=0}^{m-1} \frac{1}{\vartheta^n n!} (t^\vartheta - a^\vartheta)^n \left[\left(s^{1-\theta} \frac{d}{ds} \right)^n \omega(s) \right] \Big|_{s=a}.$$

Next, we assume that the initial value problems (3.13) and (3.14) has a unique solution in $[a, T]$, this interval is then partitioned into sub-intervals $\{[t_\sigma, t_{\sigma+1}], \sigma = 0, 1, 2, \dots, N - 1\}$, we adopt the grid points

$$t_{\sigma+1} = (t_\sigma^\vartheta + h)^{1/\vartheta}, \quad \sigma = 0, 1, 2, \dots, N - 1,$$

where $t_0 = a$ and $h = (T^\vartheta - a^\vartheta)/N$, n is the number of collocation points. By following the procedures given in [34], we have the following scheme

$$\omega_{\sigma+1} = \mu(t_{\sigma+1}) + \frac{\vartheta^{-\theta} h^\theta}{\Gamma(\theta + 2)} \sum_{j=0}^{\sigma} a_{j, \sigma+1} g(t_j, \omega_j) + \frac{\vartheta^{-\theta} h^\theta}{\Gamma(\theta + 2)} g(t_{\sigma+1}, \omega_{\sigma+1}^p), \tag{3.16}$$

where $\omega_j \equiv \omega(t_j)$ for $j = 0, 1, 2, \dots, \sigma$, and $\omega_{\sigma+1}^p$ denotes the predictor evaluated as

$$\omega_{\sigma+1}^p = \mu(t_{\sigma+1}) + \frac{\vartheta^{-\theta} h^\theta}{\Gamma(\theta + 1)} \sum_{j=0}^{\sigma} b_{j, \sigma+1} g(t_j, \omega(t_j)), \tag{3.17}$$

the weights are calculated as

$$a_{j, \sigma+1} = \begin{cases} \sigma^{\theta+1} - (\sigma - \theta)(\sigma + 1)^\theta & \text{for } j = 0, \\ 0(\sigma - j + 2)^{\theta+1} + (\sigma - j)^{\theta+1} - 2(\sigma - j + 1)^{\theta+1} & \text{for } 1 \leq j \leq \sigma, \end{cases} \tag{3.18}$$

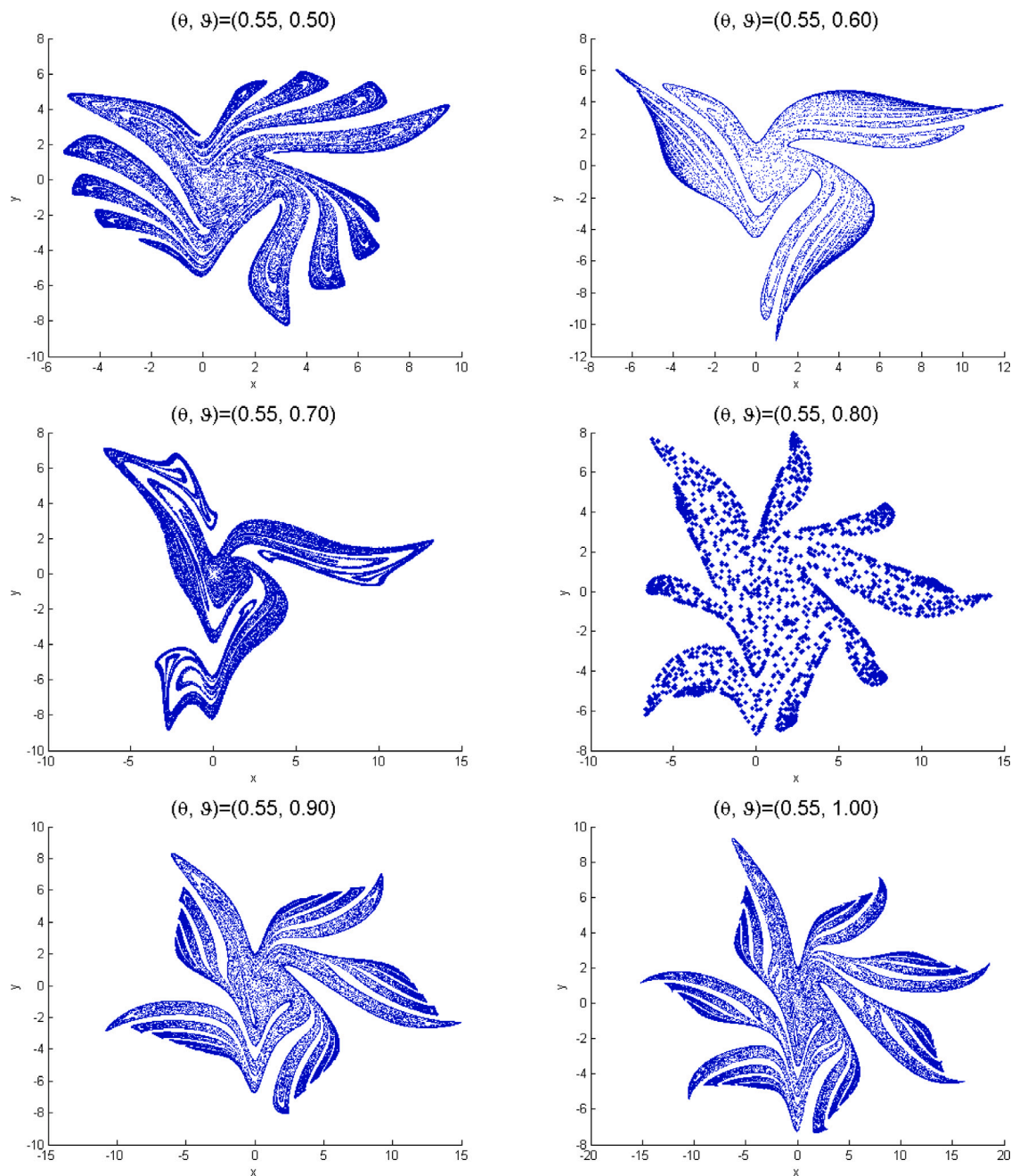


Fig. 2. Numerical simulation for the Oiseau mythique system (4.19) with varying ϑ and fixed θ at $t = 10000$.

and

$$b_{j,\sigma+1} = (\sigma + 1 - j)^\theta - (\sigma - j)^\theta.$$

Applicability and suitability of the predictor–corrector methods (3.16) and (3.17) will be tested on some generalized Caputo-type fractional chaotic systems in the next section.

Application to chaotic maps problems

In this segment, we test the suitability of the proposed generalized Caputo-type fractional derivative operator to model the Oiseau mythique Bicéphale, Oiseau mythique and L'Oiseau du paradis maps which can be found as classical-order systems in [32], these chaotic maps were presented in Paris in 1976 on international colloquium.

We adapt the predictor–corrector scheme and provide numerical results to those nonlinear chaotic models at specified values of θ and ϑ . All numerical computations are performed with the Matlab 2019a software.

Oiseau mythique map system

Consider the generalized Caputo-type fractional Oiseau mythique system

$$\begin{aligned} C_{0+}^{\theta,\vartheta} x(t) &= y(t) + \alpha(1 - 0.05y^2(t))y(t) + \mu x(t) + \frac{2(1 - \mu)x^2(t)}{1 + x^2(t)}, \\ C_{0+}^{\theta,\vartheta} y(t) &= -x(t) + \mu x(t) + \frac{2(1 - \mu)x^2(t)}{1 + x^2(t)}, \end{aligned} \tag{4.19}$$

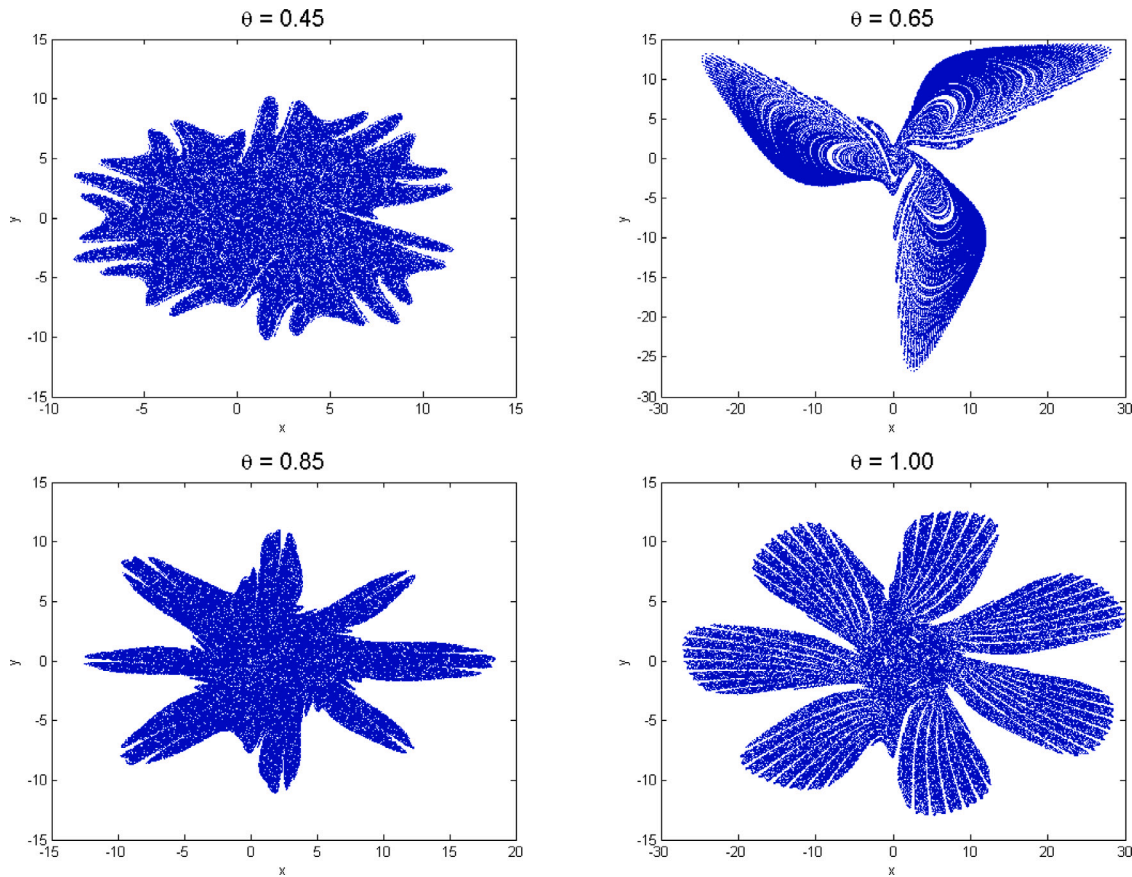


Fig. 3. Numerical simulation for the Oiseau mythique system (4.19) with varying θ , $\vartheta = 0.99$ and $\alpha = 0.08$ at $t = 10000$.

subject to initial conditions $x(0) = x_0$ and $y(0) = y_0$, where $C\mathcal{D}_{a+}^{\theta, \vartheta}$ is the new generalized Caputo fractional derivative involving the parameters θ and ϑ , such that $0 < \theta \leq 1$ and $\vartheta > 0$, μ and α are constants. By adapting the predictor–corrector algorithm as discussed in Section “Predictor–corrector method” above, the approximations $x_{\sigma+1}$ and $y_{\sigma+1}$, the generalized Caputo-type fractional Oiseau mythique system can be solve using the rules, for $N \in \mathbb{N}$ and $T > 0$,

$$\begin{aligned}
 x_{\sigma+1} &= x_0 + \frac{\vartheta^{-\theta} h^\theta}{\Gamma(\theta + 2)} \sum_{j=0}^{\sigma} a_{j, \sigma+1} \\
 &\times \left(y_j + \alpha(1 - 0.05y_j^2)y(t) + \mu x_j + \frac{2(1 - \mu)x_j^2}{1 + x_j^2} \right) \\
 &+ \frac{\vartheta^{-\theta} h^\theta}{\Gamma(\theta + 2)} \left(y_{\sigma+1}^p + \alpha(1 - 0.05(y_{\sigma+1}^p)^2)y_{\sigma+1}^p + \mu x_{\sigma+1}^p \right. \\
 &\left. + \frac{2(1 - \mu)(x_{\sigma+1}^p)^2}{1 + (x_{\sigma+1}^p)^2} \right) \\
 y_{\sigma+1} &= y_0 - \frac{\vartheta^{-\theta} h^\theta}{\Gamma(\theta + 2)} \sum_{j=0}^{\sigma} a_{j, \sigma+1} \left(x_j + \mu x_j + \frac{2(1 - \mu)x_j^2}{1 + x_j^2} \right), \\
 &- \frac{\vartheta^{-\theta} h^\theta}{\Gamma(\theta + 2)} \left(x_{\sigma+1}^p + \mu x_{\sigma+1}^p + \frac{2(1 - \mu)(x_{\sigma+1}^p)^2}{1 + (x_{\sigma+1}^p)^2} \right),
 \end{aligned}
 \tag{4.20}$$

where $h = \frac{T^\vartheta}{N}$ and predictors are calculated as

$$\begin{aligned}
 x_{\sigma+1}^p &= x_0 + \frac{\vartheta^{-\theta} h^\theta}{\Gamma(\theta + 1)} \sum_{j=0}^{\sigma} b_{j, \sigma+1} \\
 &\times \left(y_j + \alpha(1 - 0.05y_j^2)y(t) + \mu x_j + \frac{2(1 - \mu)x_j^2}{1 + x_j^2} \right), \\
 y_{\sigma+1}^p &= y_0 - \frac{\vartheta^{-\theta} h^\theta}{\Gamma(\theta + 1)} \sum_{j=0}^{\sigma} b_{j, \sigma+1} \left(x_j + \mu x_j + \frac{2(1 - \mu)x_j^2}{1 + x_j^2} \right).
 \end{aligned}
 \tag{4.21}$$

With $\mu = -0.496$, $\alpha = 0.008$, $x_0 = 0.5$ and $y_0 = 0.5$, the generalized Caputo-type fractional Oiseau mythique system (4.19) displays some chaotic attractors in Figs. 1–3 for different values of θ and ϑ , as shown in the captions. Further, we slightly perturbed the parameters μ and α , as $\mu = \cos(4\pi i/5) + 0.008$ and $\alpha = 0.009$ to obtain chaotic phenomena as displayed in Fig. 4 for some values of θ and ϑ . Plots (a–f) correspond to $\vartheta = \vartheta = 1.15$ and $\theta = (0.41, 0.48, 0.53, 0.90, 0.74, 0.95)$, respectively. It was observed in the simulation process that for system (4.19) to give rise to chaotic behaviors, the sum of θ and ϑ must be greater than or equal to one, if otherwise no attractor is achieved.

Oiseau mythique Bicéphale map system

For the second example, we consider the Oiseau mythique Bicéphale system [32], which is modeled in this case with the generalized Caputo-type fractional derivative in the form

$$\begin{aligned}
 C\mathcal{D}_{0+}^{\theta, \vartheta} x(t) &= y(t) + \mu x(t) + \frac{2(1 - \mu)x^2(t)}{1 + x^4(t)} + \alpha(1 - \beta(y^2(t) + 3x^2(t)))y(t), \\
 C\mathcal{D}_{0+}^{\theta, \vartheta} y(t) &= -x(t) + \mu x(t) + \frac{2(1 - \mu)x^2(t)}{1 + x^4(t)},
 \end{aligned}
 \tag{4.22}$$

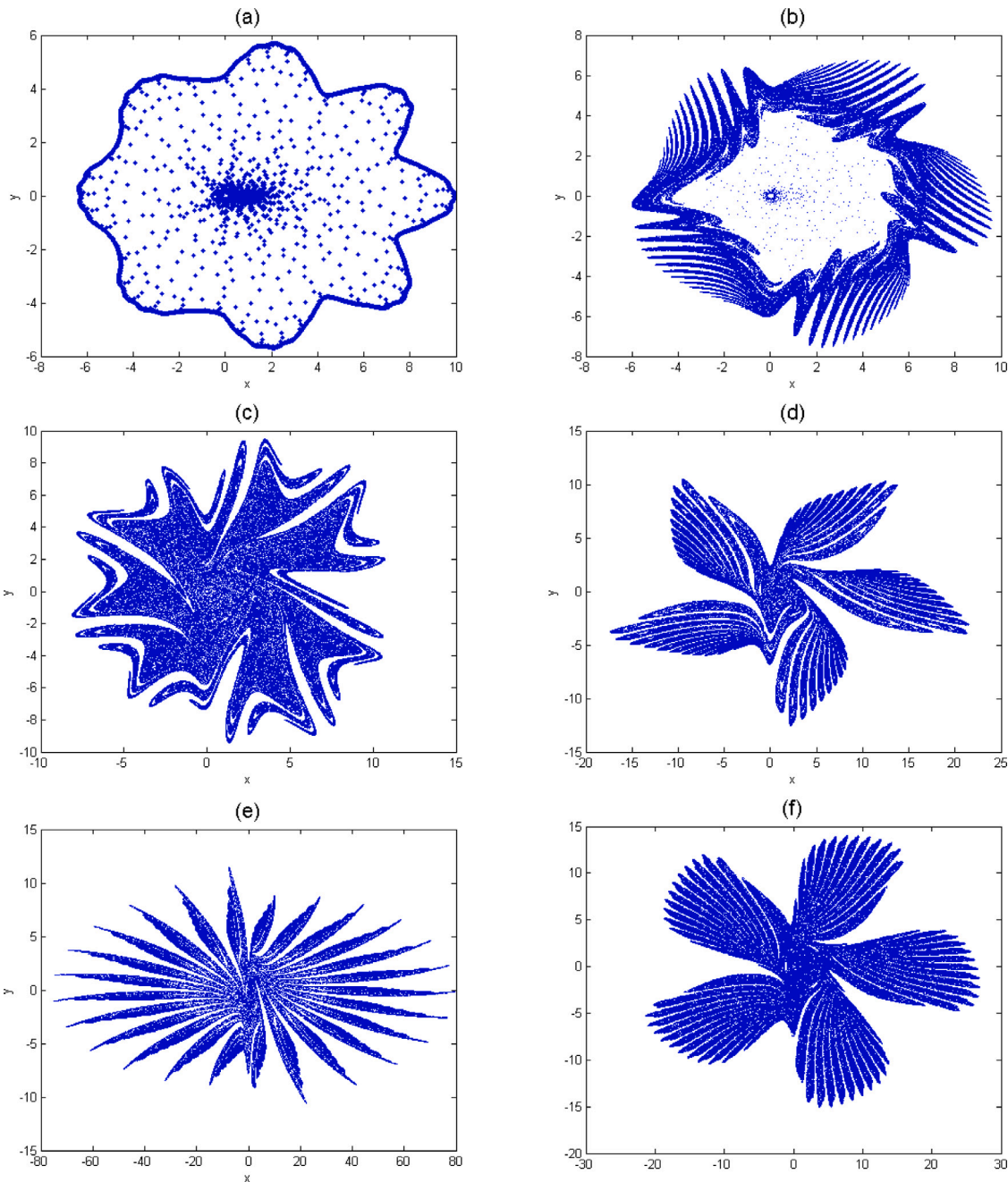


Fig. 4. Numerical simulation for the Oiseau mythique system (4.19) with different values of ϑ and θ at $t = 150000$. Here, $\mu = \cos(4\pi/5) + 0.008$ and $\alpha = 0.009$.

where μ, α and β are parameters to be given. By applying the predictor-corrector scheme to (4.22), we have

$$\begin{aligned}
 x_{\sigma+1} &= x_0 + \frac{\vartheta^{-\theta} h^\theta}{\Gamma(\theta+2)} \sum_{j=0}^{\sigma} a_{j,\sigma+1} \left\{ y_j + \mu x_j + \frac{2(1-\mu)x_j^2}{1+x_j^4} + \alpha(1-\beta(y_j^2+3x_j^2))y_j \right\} \\
 &+ \frac{\vartheta^{-\theta} h^\theta}{\Gamma(\theta+2)} \left\{ y_{\sigma+1}^p + \mu x_{\sigma+1}^p + \frac{2(1-\mu)(x_{\sigma+1}^p)^2}{1+(x_{\sigma+1}^p)^4} \right. \\
 &\quad \left. + \alpha(1-\beta((y_{\sigma+1}^p)^2+3(x_{\sigma+1}^p)^2))y_{\sigma+1}^p \right\}, \\
 y_{\sigma+1} &= y_0 + \frac{\vartheta^{-\theta} h^\theta}{\Gamma(\theta+2)} \sum_{j=0}^{\sigma} a_{j,\sigma+1} \left\{ -x_j + \mu x_j + \frac{2(1-\mu)x_j^2}{1+x_j^4} \right\} \\
 &+ \frac{\vartheta^{-\theta} h^\theta}{\Gamma(\theta+2)} \left\{ -x_{\sigma+1}^p + \mu x_{\sigma+1}^p + \frac{2(1-\mu)(x_{\sigma+1}^p)^2}{1+(x_{\sigma+1}^p)^4} \right\},
 \end{aligned}
 \tag{4.23}$$

where h remains as earlier defined, and

$$\begin{aligned}
 x_{\sigma+1}^p &= x_0 + \frac{\vartheta^{-\theta} h^\theta}{\Gamma(\theta+1)} \sum_{j=0}^{\sigma} b_{j,\sigma+1} \\
 &\times \left\{ y_j + \mu x_j + \frac{2(1-\mu)x_j^2}{1+x_j^4} + \alpha(1-\beta(y_j^2+3x_j^2))y_j \right\}, \\
 y_{\sigma+1}^p &= y_0 + \frac{\vartheta^{-\theta} h^\theta}{\Gamma(\theta+1)} \sum_{j=0}^{\sigma} b_{j,\sigma+1} \left\{ -x_j + \mu x_j + \frac{2(1-\mu)x_j^2}{1+x_j^4} \right\},
 \end{aligned}
 \tag{4.24}$$

With $\mu = 0.325, \beta = 0.01$, and $\alpha = 0.0025$, system (4.22) gives chaotic oscillations for various values of θ and ϑ as presented in Fig. 5. The initial conditions are specified as $x_0 = 0.1$ and $y_0 = 0.1$. Also, with $\alpha = 0.00025, \vartheta = 1.25$, chaotic phenomena in Fig. 6 is obtained.

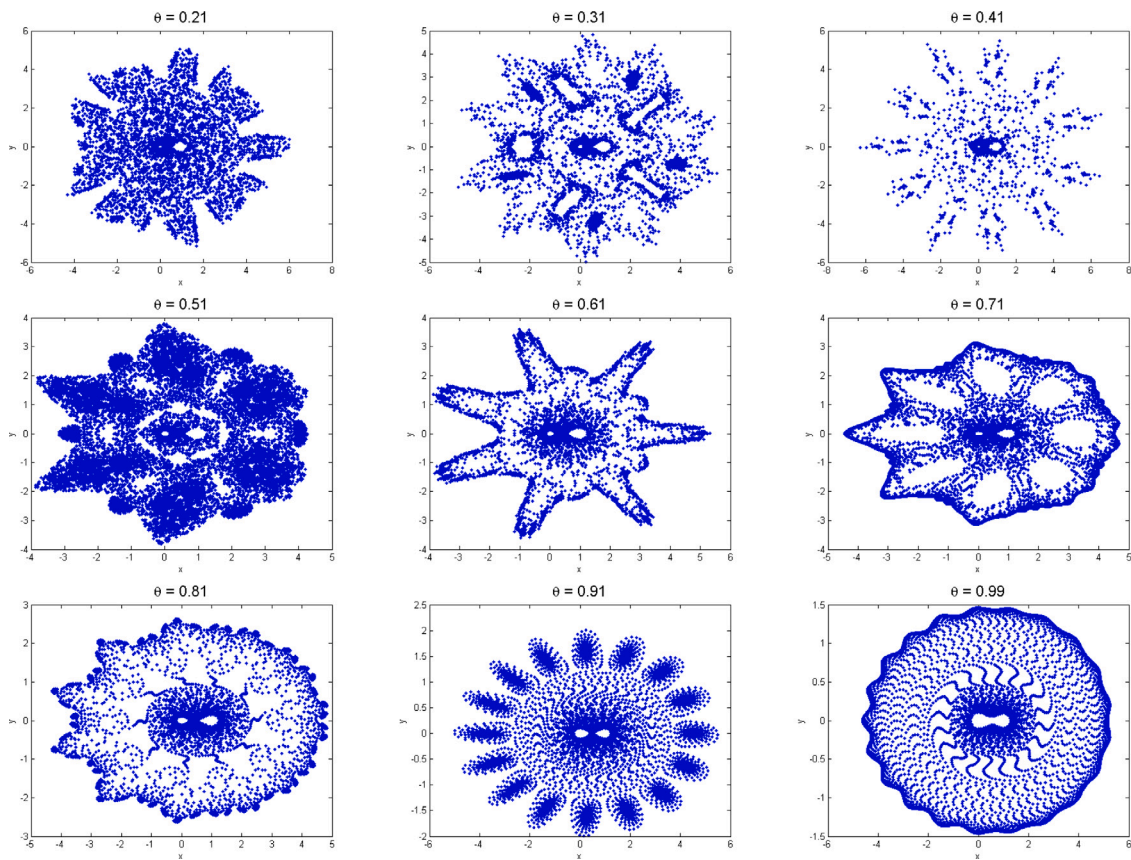


Fig. 5. Numerical simulation for the Oiseau mytique Bicéphale map system (4.22) for different values of θ and $\vartheta = 0.98$. Simulation runs for $t = 500\,000$.

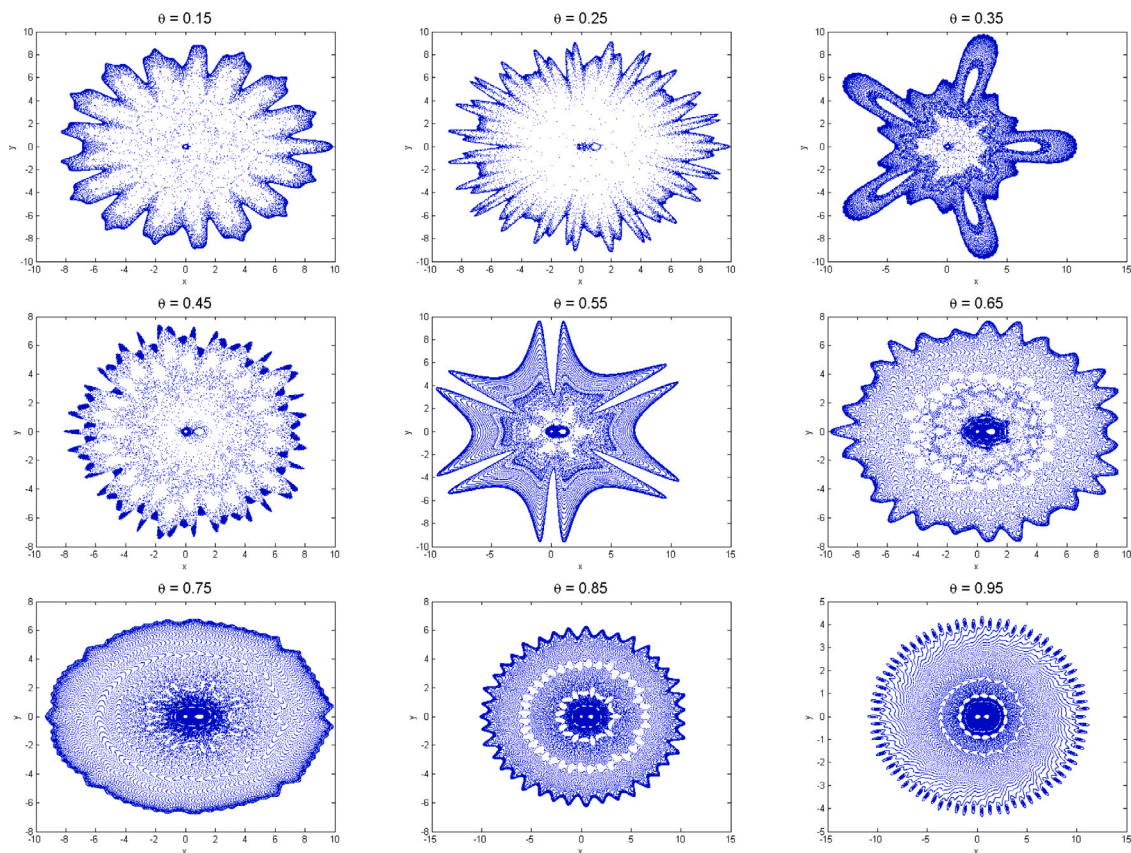


Fig. 6. Numerical results showing the attractors for system (4.22) at different instances of θ . Simulation runs for $t = 500\,000$.

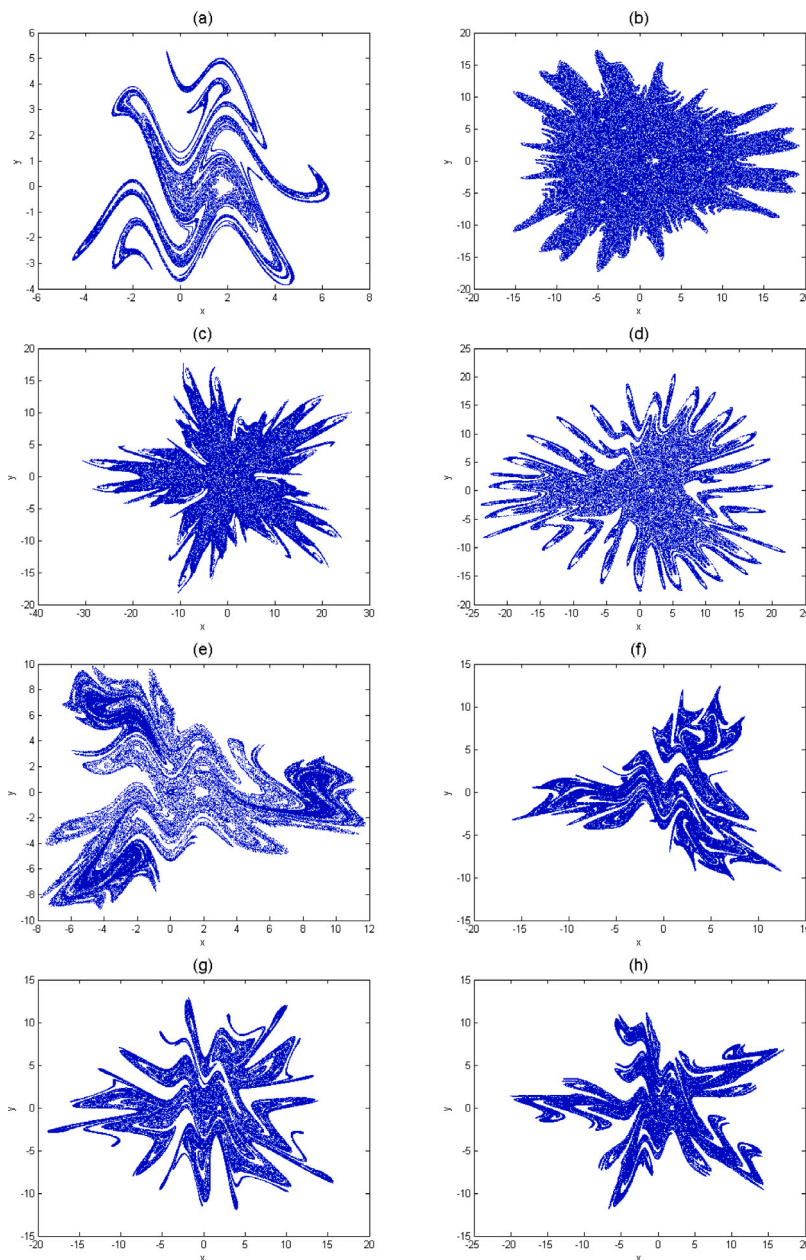


Fig. 7. Numerical simulation showing chaotic evolution for the Oiseau du paradis system (4.25) for different parameter values with $\theta = 0.99$ and $\theta = 0.99$.

L'Oiseau du paradis system

The third example covers the generalized Caputo-type L'Oiseau du paradis fractional system

$${}^C \mathcal{D}_{0+}^{\theta, \theta} x(t) = y(t) + \alpha y^2(t)(1 - \beta y^2(t)) + \mu x(t) + (1 - \mu)x^2(t) \times \exp\left(\frac{1 - x^2(t)}{4}\right) \tag{4.25}$$

$${}^C \mathcal{D}_{0+}^{\theta, \theta} y(t) = -x(t) + \mu x(t) + (1 - \mu)x^2(t) \exp\left(\frac{1 - x^2(t)}{4}\right),$$

which can be written in the predictor–corrector mode as

$$x_{\sigma+1} = x_0 + \frac{\theta^{-\theta} h^\theta}{\Gamma(\theta + 2)} \sum_{j=0}^{\sigma} a_{j, \sigma+1} \times \left[y_j + \alpha y_j^2(1 - \beta y_j^2) + \mu x_j + (1 - \mu)x_j^2 \exp\left(\frac{1 - x_j^2}{4}\right) \right]$$

$$+ \frac{\theta^{-\theta} h^\theta}{\Gamma(\theta + 2)} \left\{ y_{\sigma+1}^p + \alpha(y_{\sigma+1}^p)^2(1 - \beta(y_{\sigma+1}^p)^2) + \mu x_{\sigma+1}^p + (1 - \mu)(x_{\sigma+1}^p)^2 \exp\left(\frac{1 - (x_{\sigma+1}^p)^2}{4}\right) \right\},$$

$$y_{\sigma+1} = y_0 + \frac{\theta^{-\theta} h^\theta}{\Gamma(\theta + 2)} \sum_{j=0}^{\sigma} a_{j, \sigma+1} \left[-x_j + \mu x_j + (1 - \mu)x_j^2 \exp\left(\frac{1 - x_j^2}{4}\right) \right]$$

$$+ \frac{\theta^{-\theta} h^\theta}{\Gamma(\theta + 2)} \left\{ -x_{\sigma+1}^p + \mu x_{\sigma+1}^p + (1 - \mu)(x_{\sigma+1}^p)^2 \times \exp\left(\frac{1 - (x_{\sigma+1}^p)^2}{4}\right) \right\},$$

(4.26)

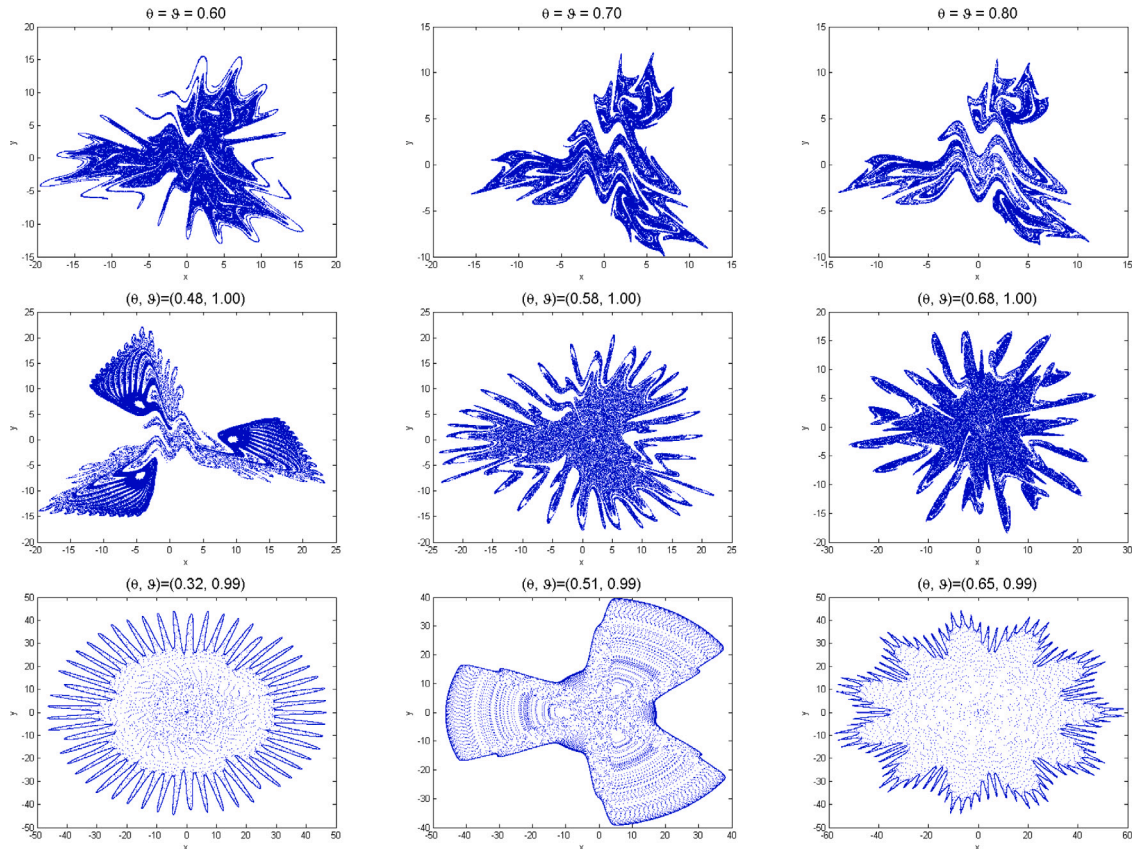


Fig. 8. Chaotic attractors for Oiseau du paradis system (4.25) for different values of θ and ϑ , other parameters are: $\mu = -0.48, \beta = 0.1, \alpha = 0.018$. Simulation runs for $t = 100000$.

where

$$\begin{aligned}
 x_{\sigma+1}^p &= x_0 + \frac{\vartheta^{-\theta} h^\theta}{\Gamma(\theta+1)} \sum_{j=0}^{\sigma} b_{j,\sigma+1} \left\{ y_j + \alpha y_j^2 (1 - \beta y_j^2) + \mu x_j + (1 - \mu) x_j^2 \right. \\
 &\quad \left. \times \exp\left(\frac{1 - x_j^2}{4}\right) \right\}, \\
 y_{\sigma+1}^p &= y_0 + \frac{\vartheta^{-\theta} h^\theta}{\Gamma(\theta+1)} \sum_{j=0}^{\sigma} b_{j,\sigma+1} \left\{ -x_j + \mu x_j + (1 - \mu) x_j^2 \exp\left(\frac{1 - x_j^2}{4}\right) \right\}.
 \end{aligned}
 \tag{4.27}$$

With the initial conditions $x_0 = 0.1, y_0 = 0$ and specific parameter values as specified in Figs. 7 and 8, the generalized Caputo-type fractional L'Oiseau du paradis model (4.25) displayed some chaotic behaviors. In Fig. 7, the parameters correspond to (a) $\mu = -0.38, \beta = 1, \alpha = 0.018$, (b) $\mu = -0.38, \beta = 0.01, \alpha = 0.0018$, (c) $\mu = -0.78, \beta = 0.01, \alpha = 0.018$, (d) $\mu = -0.58, \beta = 0.01, \alpha = 0.018$, (e) $\mu = -0.40, \beta = 0.1, \alpha = 0.0083$, (f) $\mu = -0.58, \beta = 0.1, \alpha = 0.0083$, (g) $\mu = -0.68, \beta = 0.1, \alpha = 0.0083$ and (h) $\mu = -0.78, \beta = 0.1, \alpha = 0.0083$ with varying and $\alpha = 0.08$ at $t = 100000$, the values of θ and ϑ are given in the caption.

The Gumowski–Mira map

To extend the numerical examples in this work, we consider the Gumowski–Mira chaotic system [36,37] written in the predictor–corrector mode with the generalized Caputo-type operator as

$$\begin{aligned}
 x_{\sigma+1} &= x_0 + \frac{\vartheta^{-\theta} h^\theta}{\Gamma(\theta+2)} \sum_{j=0}^{\sigma} a_{j,\sigma+1} \left[y_j + \alpha (1 - \gamma y_j^2) + \beta x_j + \frac{2x_j^2(1 - \beta)}{(1 + x_j^2)} \right] \\
 &\quad + \frac{\vartheta^{-\theta} h^\theta}{\Gamma(\theta+2)} \left\{ y_{\sigma+1}^p + \alpha (1 - \gamma (y_{\sigma+1}^p)^2) + \beta x_{\sigma+1}^p + \frac{2(x_{\sigma+1}^p)^2(1 - \beta)}{(1 + (x_{\sigma+1}^p)^2)} \right\}, \\
 y_{\sigma+1} &= y_0 + \frac{\vartheta^{-\theta} h^\theta}{\Gamma(\theta+2)} \sum_{j=0}^{\sigma} a_{j,\sigma+1} \left[-x_j + \beta x_j + \frac{2x_j^2(1 - \beta)}{(1 + x_j^2)} \right] \\
 &\quad + \frac{\vartheta^{-\theta} h^\theta}{\Gamma(\theta+2)} \left\{ -x_{\sigma+1}^p + \beta x_{\sigma+1}^p + \frac{2(x_{\sigma+1}^p)^2(1 - \beta)}{(1 + (x_{\sigma+1}^p)^2)} \right\},
 \end{aligned}
 \tag{4.28}$$

where

$$\begin{aligned}
 x_{\sigma+1}^p &= x_0 + \frac{\vartheta^{-\theta} h^\theta}{\Gamma(\theta+1)} \sum_{j=0}^{\sigma} b_{j,\sigma+1} \left\{ y_j + \alpha (1 - \gamma y_j^2) + \beta x_j + \frac{2x_j^2(1 - \beta)}{(1 + x_j^2)} \right\}, \\
 y_{\sigma+1}^p &= y_0 + \frac{\vartheta^{-\theta} h^\theta}{\Gamma(\theta+1)} \sum_{j=0}^{\sigma} b_{j,\sigma+1} \left\{ -x_j + \beta x_j + \frac{2x_j^2(1 - \beta)}{(1 + x_j^2)} \right\}.
 \end{aligned}
 \tag{4.29}$$

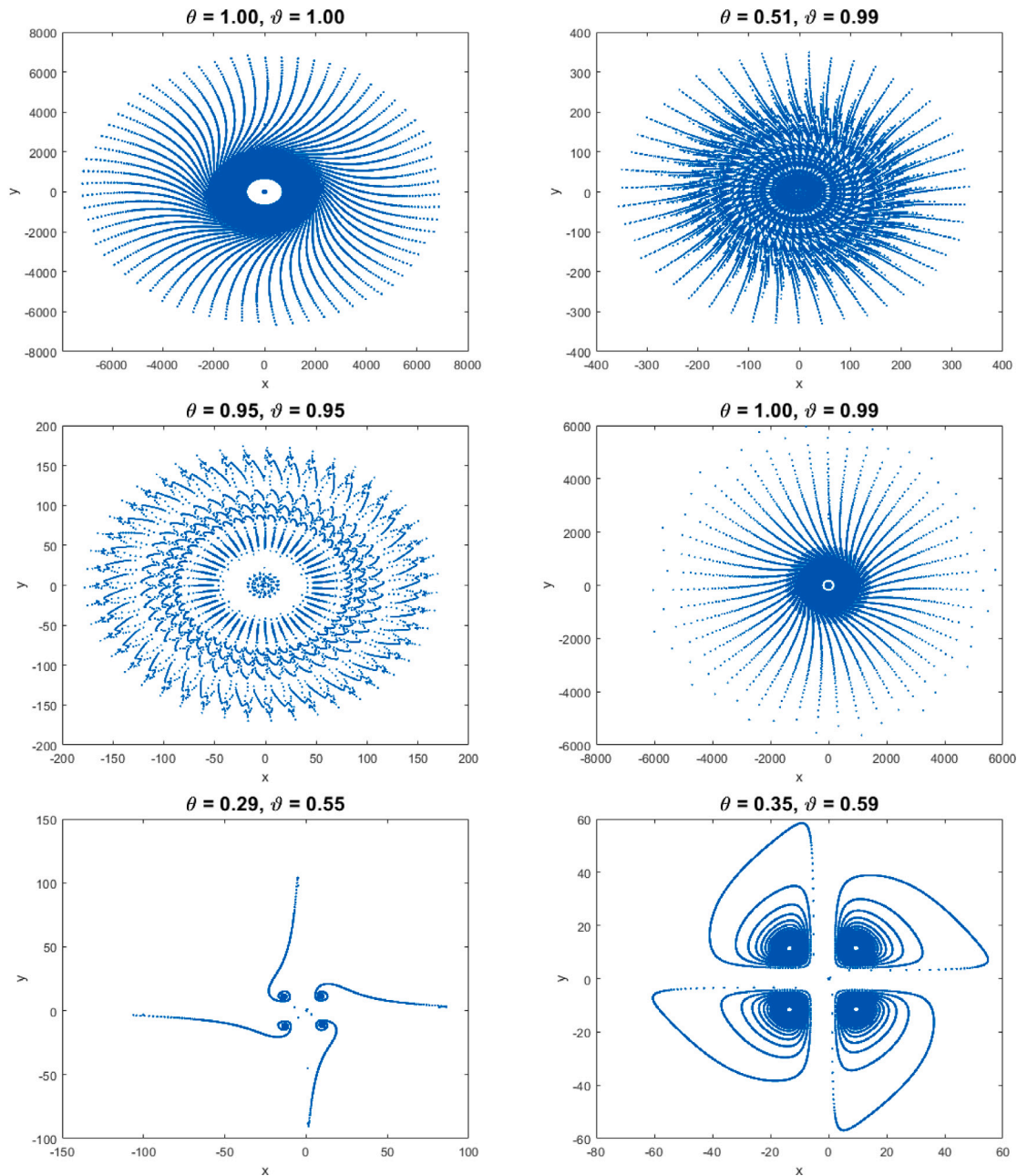


Fig. 9. Chaotic evolution fractional Gumowski-Mira map (4.28) for different values θ and ϑ .

subject to initial conditions $x_0 = 5, y_0 = 0$, and parameters $\alpha = 0.003, \beta = 0.1$ and $\gamma = 0.005$. Numerical experiments are repeated for different values of ϑ and θ as shown in Fig. 9.

The multi-fold Henon map

Finally, we give an extension here by considering the generalized Caputo-type Hellon map dynamics [37,38] via the predictor-corrector schemes as

$$\begin{aligned}
 x_{\sigma+1} &= x_0 + \frac{\vartheta^{-\theta} h^\theta}{\Gamma(\theta+2)} \sum_{j=0}^{\sigma} a_{j,\sigma+1} [1 - \alpha \sin(x_j) + \beta y_j], \\
 &+ \frac{\vartheta^{-\theta} h^\theta}{\Gamma(\theta+2)} \left\{ 1 - \alpha \sin(x_{\sigma+1}^p) + \beta y_{\sigma+1}^p \right\}, \\
 y_{\sigma+1} &= y_0 + \frac{\vartheta^{-\theta} h^\theta}{\Gamma(\theta+2)} \sum_{j=0}^{\sigma} a_{j,\sigma+1} [x_j] + \frac{\vartheta^{-\theta} h^\theta}{\Gamma(\theta+2)} \left\{ x_{\sigma+1}^p \right\},
 \end{aligned}
 \tag{4.30}$$

where

$$\begin{aligned}
 x_{\sigma+1}^p &= x_0 + \frac{\vartheta^{-\theta} h^\theta}{\Gamma(\theta+1)} \sum_{j=0}^{\sigma} b_{j,\sigma+1} \{ 1 - \alpha \sin(x_j) + \beta y_j \}, \\
 y_{\sigma+1}^p &= y_0 + \frac{\vartheta^{-\theta} h^\theta}{\Gamma(\theta+1)} \sum_{j=0}^{\sigma} b_{j,\sigma+1} \{ x_j \}.
 \end{aligned}
 \tag{4.31}$$

We utilize the initial condition and parameters $x_0 = 5, y_0 = 0, \alpha = 0.48$ and $\beta = 0.9924$ to obtain the dynamic behaviors in Fig. 10 for some instances of θ and ϑ

Conclusion

Application of the new generalized Caputo-type fractional derivative operator to model the two-dimensional form of the generalized Oiseau mythique map, L'Oiseau du paradis and the Oiseau mythique

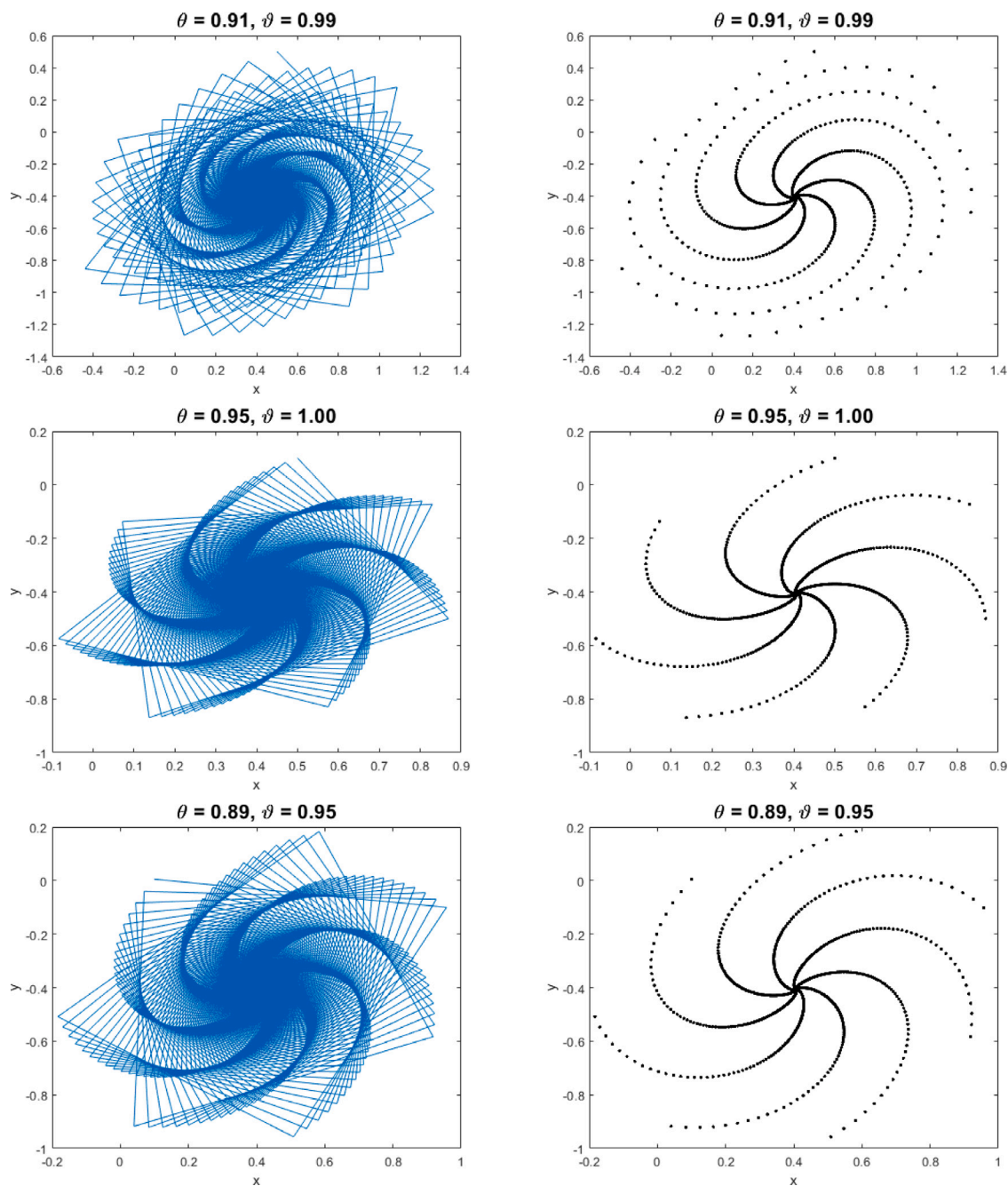


Fig. 10. Chaotic dynamics of fractional Henon system (4.30) for different values θ and ϑ .

Bicéphale map systems are considered in this paper. The new generalized Caputo-type operator is approximated by the novel predictor-corrector algorithm. The simulation results obtained for different instances of θ and ϑ showed that the fractional maps displayed very strange complex (chaotic) dynamical behaviors due to memory and the order of the new operator. These features make the fractional-order chaotic maps system to be distinctive from the known classical-order maps. In addition, based on the dynamical behaviors that evolved during the computational experiments, one could opined that the fractional-order systems have higher complexity when compared to the classical-order models, which implies that the two-dimensional generalized Caputo-type fractional-order maps have better application

prospects than its corresponding standard order representations. Application of the numerical techniques and the new fractional derivative to models in engineering and sciences will be the future research direction.

CRediT authorship contribution statement

Kolade M. Owolabi: The idea in the manuscript was conceived, Initial draft was made, Computation was carried out using the Matlab software, Final draft was proofread and approved. **Edson Pindza:** The idea in the manuscript was conceived, Supervision, Computation was carried out using the Matlab software, Final draft was proofread and approved.

Declaration of competing interest

The authors declare that they have no known competing financial interests or personal relationships that could have appeared to influence the work reported in this paper.

References

- [1] Podlubny I. Fractional differential equations. San Diego: Academic Press; 1999.
- [2] Kilbas AA, Srivastava HM, Trujillo JJ. Theory and applications of fractional differential equations. Netherlands: Elsevier; 2006.
- [3] Diethelm K. The analysis of fractional differential equations: An application-oriented exposition using differential operators of Caputo type. Springer lecture notes in mathematics, Berlin Heidelberg: Springer-Verlag; 2010.
- [4] Miller KS, Ross B. An introduction to the fractional calculus and fractional differential equations. New York, NY, USA: John Wiley & Sons; 1993.
- [5] Oldham KB, Spanier J. The fractional calculus: Theory and applications of differentiation and integration to arbitrary order. New York: Dover Publication; 2006.
- [6] Owolabi KM, Atangana A. Numerical methods for fractional differentiation. Singapore: Springer; 2019.
- [7] Atangana A. On the new fractional derivative and application to nonlinear Fisher's reaction–diffusion equation. Appl Math Comput 2016;273:948–56.
- [8] Atangana A, Qureshi S. Modeling attractors of chaotic dynamical systems with fractal–fractional operators. Chaos Solitons Fractals 2019;123:320–37.
- [9] Atangana A, Akgul A, Owolabi KM. Analysis of fractal fractional differential equations. Alex Eng J 2020;59:1117–34.
- [10] Roohi M, Aghababa MP, Haghghi AR. Switching adaptive controllers to control fractional-order complex systems with unknown structure and input nonlinearities. Complexity 2015;21:211–23.
- [11] Roohi M, Zhang C, Chen Y. Adaptive model-free synchronization of different fractional-order neural networks with an application in cryptography. Nonlinear Dynam 2020;100:3979–4001.
- [12] Owolabi KM, Karaagac B. Chaotic and spatiotemporal oscillations in fractional reaction–diffusion system. Chaos Solitons Fractals 2020;141:110302.
- [13] Qureshi S, Atangana A. Fractal-fractional differentiation for the modeling and mathematical analysis of nonlinear diarrhea transmission dynamics under the use of real data. Chaos Solitons Fractals 2010;136:109812.
- [14] Qureshi S, Atangana A, Shaikh AA. Strange chaotic attractors under fractal-fractional operators using newly proposed numerical methods. Eur Phys J Plus 2019;134:523.
- [15] Peng Y, He S, Sun K. Chaos in the discrete memristor-based system with fractional-order. Results Phys 2021;24:104106.
- [16] Mahmoud EE, Trikha P, Jahanzaib LS, Eshmawi AA, Matoog RT. Chaos control and penta-compound combination anti-synchronization on a novel fractional chaotic system with analysis and application. Results Phys 2021;24:104130.
- [17] Strogatz SH. Nonlinear dynamics and chaos: With application to physics, biology, chemistry and engineering. Reading MA: Addison-Wesley; 1994.
- [18] Avalos-Ruiz LF, Gomez-Aguilar JF, Atangana A, Owolabi KM. On the dynamics of fractional map with power-law, exponential decay and Mittag-Leffler memory. Chaos Solitons Fractals 2019;127:364–88.
- [19] Owolabi KM, Gomez-Aguilar JF, Fernandez-Anaya G, Lavin-Delgado JE, Hernandez-Castillo E. Modelling of chaotic processes with Caputo fractional order derivative. Entropy 2020;22:1027.
- [20] Naik PA, Owolabi KM, Yavuz M, Zu J. Chaotic dynamics of fractional order HIV-1 model involving AIDS-related cancer cells. Chaos Solitons Fractals 2020;140:110272.
- [21] Owolabi KM. Numerical approach to chaotic pattern formation in diffusive predator–prey system with Caputo fractional operator. Numer Methods Partial Differential Equations 2020;1–21.
- [22] Yang SK, Chen CL, Yau HT. Control of chaos in lorenz system. Chaos Solitons Fractals 2007;33:1367–75.
- [23] Wu T, Chen MS. Chaos control of the modified Chua's circuit system. Physica D 2002;164:53–8.
- [24] Owolabi KM. Riemann–Liouville fractional derivative and application to model chaotic differential equations. Prog Fract Differ Appl 2018;4:99–110.
- [25] Yassen MT. Chaos control of chen chaotic dynamical system. Chaos Solitons Fractals 2003;15:271–83.
- [26] Matouk AE. Dynamical analysis, feedback control and synchronization of liu dynamical system. Nonlinear Anal: Theory Method Appl 2008;69:162–72.
- [27] Owolabi KM, Gomez-Aguilar JF, Karaagac B. Modelling, analysis and simulations of some chaotic systems using derivative with Mittag-Leffler kernel. Chaos Solitons Fractals 2019;125:54–63.
- [28] Al-Khedhairi A, Matouk AE, Askar SS. Computations of synchronisation conditions in some fractional-order chaotic and hyperchaotic systems. Pramana 2019;92:1–222.
- [29] Zhou C, Li Z, Zeng Y, Zhang S. A novel 3d fractional-order chaotic system with multifarious coexisting attractors. Int J Bifurcation Chaos 2019;29:1–19.
- [30] Gholamin P, Sheikhan AR. Dynamical analysis of a new three-dimensional fractional chaotic system. Pramana 2019;92:1–9.
- [31] Zhou C, Li Z, Xie F. Coexisting attractors, crisis route to chaos in a novel 4d fractional-order system and variable-order circuit implementation. Eur Phys J Plus 2019;134:1–17.
- [32] Abraham R, Ueda Y. The chaos avant-garde: Memories of the early days of chaos theory, Vol. 39. World Scientific; 2000.
- [33] Katugampola UN. Existence and uniqueness results for a class of generalized fractional differential equations. 2014, arXiv:1411.5229.
- [34] Odibat Z, Baleanu D. Numerical simulation of initial value problems with generalized Caputo-type fractional derivatives. Appl Numer Math 2020;156:94–105.
- [35] Osler TJ. Leibniz rule for fractional derivatives generalized and an application to infinite series. SIAM J Appl Math 1970;18:658–74.
- [36] Gumowski I, Mura C. Recurrences and discrete dynamic systems. Berlin: Springer-Verlag; 1980.
- [37] Morris WH, Stephen S, Robert LD. Differential equations, dynamical systems, and an introduction to chaos. New York: Academic Press; 2013.
- [38] Henon M. A two-dimensional mapping with strange attractor. Comm Math Phys 1976;50.